Anomalous thresholds and the realization of chiral symmetry*

J. J. Brehm

Department of Physics and Astronomy, University of Massachusetts, Amherst, Massachusetts 01002

(Received 26 March 1973; revised manuscript received 16 July 1973)

We follow the work of some other authors in a study of chiral-symmetry breaking based on the linear σ model in the semiclassical approximation. By this procedure the masses of the mesons are known in terms of the symmetry-breaking parameters. Therefore, in those terms, we can analyze the system for the possible occurrence of anomalous thresholds corresponding to the bound-state properties of the scalar mesons. We find that when the critical parameter in the symmetric Lagrangian is such that a Goldstone symmetry limit can occur, then the anomalous threshold does not manifest itself by emerging to the physical sheet when mass continuation is performed; instead, the anomalous singularity stays out on the physical sheet and never disappears from it. Conversely, the system has an anomalous threshold with familiar emerging behavior when the critical parameter admits only the normal symmetry limit.

I. INTRODUCTION

Underlying the many applications of current algebra is the assumed validity of an approximate chiral symmetry of the hadrons. The convictions are that the real world is not far removed from one in which all the vector and axial-vector currents are conserved, and that the fully chiral-symmetric situation is one in which there occur massless Goldstone bosons rather than degenerate chiral multiplets. This question of how the symmetry limit is realized can be studied in models, and Olshansky[1] has examined the linear σ model[2] for this purpose. The same model has been employed by Carruthers and Haymaker[3] (CH) to study a number of issues related to chiral-symmetry breaking, including the one concerning how the symmetry is realized.

These authors use a chiral-symmetric meson-field Lagrangian whose parameters are thought of as fixed and symmetry breakers whose parameters can be varied to permit passage between the physical and the symmetrical configurations. They solve the model in the semiclassical approximation to obtain relations among the masses of the scalar and pseudoscalar mesons, the parameters of the symmetric Lagrangian, and the symmetry-breaking parameters. The results are quite realistic for such a simplified treatment.[4] Unfortunately it is difficult to draw a firm conclusion about the realization of the chiral-symmetry limit[1,5]; the scalar-meson spectrum is not well-enough established to fix the parameters which are sensitive in distinguishing the different modes of realizing the full symmetry. The authors of Ref. 5 identify a critical constant, related only to the parameters of the symmetric part of the Lagrangian, whose value determines whether or not it is possible for full symmetry to be realized in the Goldstone fashion.

In this paper we shall explore a further issue related to the meson spectrum. We shall have nothing to add which is decisive about the realization of chiral symmetry. Rather we shall demonstrate how the CH critical parameter plays an interesting role in certain questions of compositeness among the mesons.

We shall concentrate on the vertex in which a scalar (S) particle is coupled to a pair of pseudoscalar (P) particles. The values of the masses m_S and m_P determine three regimes describing $S \to PP$, as m_S increases relative to m_P:

$$\text{bound} \to \text{loosely bound} \to \text{unbound}.$$

The third regime obviously corresponds to instability, when $m_S^2 \geq 4m_P^2$. The distinction between the first two regimes also has a precise meaning. To express it we shall consider the form factor of the S particle: the S-to-S matrix element of any local operator which can probe the S-particle structure [see Fig. 1(a)]. The form factor is analytic in t, the momentum transfer squared. When we refer to S as bound, we mean that m_S and m_P are such that the lowest-lying cut in the t plane corresponds to the PP intermediate state[6] [Fig. 1(b)]. The $S \to PP$ coupling provides a pole term for the amplitude $SS \to PP$ [Fig. 1(c)]; corresponding to this contribution there is a branch point of the absorptive part of the form factor which, until m_S is increased, does not lie on the physical sheet of the form factor itself. The loosely bound configuration is reached as we increase m_S until $m_S^2 \geq 2m_P^2$. In this circumstance the branch point for Fig. 1(c) emerges through the PP cut onto the physical sheet [Fig. 1(d)]. Thus for $m_S^2 > 2m_P^2$ there is a form-factor branch point (the anomalous threshold) which lies lower than the PP threshold. The location of the anomalous branch point can be found from a study[7,8] of the analytic properties of diagram 1(c); it is given by

$$t_0 = m_S^2(4m_P^2 - m_S^2)/m_P^2 . \quad (1)$$

If we introduce a different variable,

$$\nu = t - 4m_P^2 ,$$

then the PP cut starts at the origin in the ν plane and the anomalous threshold occurs at

$$\nu_0 = -(m_S^2 - 2m_P^2)^2/m_P^2 ; \quad (1')$$

in this form the emergence of the anomalous threshold with increasing m_S is apparent.

For small momentum transfer the anomalous cut is dominant if it occurs. Long ago, Nambu[9] showed how its effect is to be expected. For small binding energy ϵ, (1) becomes

$$t_0 \simeq 16\epsilon m_P$$

so that the reciprocal radius of the bound state can be identified as $\simeq 4(\epsilon m_P)^{1/2}$. This corresponds to a bound-state wave function for the S particle which, at large r (the PP separation), is asymptotically $r^{-1}\exp[-r(\epsilon m_P)^{1/2}]$, as one expects from nonrelativistic quantum mechanics. Thus the anomalous threshold is a familiar property of bound states and not at all anomalous.

The final point to review in preparation for the investigation at hand relates to the analytic continuation of the form factor when the anomalous threshold makes its appearance.[10] For S bound, but not loosely bound, we have a dispersion relation for the form factor:

$$F(t) = \frac{1}{\pi}\int_{4m_P^2}^{\infty} \frac{A(t')dt'}{t' - t} ; \quad (2)$$

this is represented by the contour integral in Fig. 2(a), in which it is the absorptive part $A(t)$ which is integrated along the contour. The shaded left cut is that of A, from Fig. 1(c). As S becomes loosely bound, the singularity of A deforms the contour as shown in Fig. 2(b). The final result of the continuation for $m_S^2 > 2m_P^2$ is shown in Fig. 2(c), where formula (2) must be supplemented by the anomalous contribution in which we integrate the discontinuity of $A(t)$ from t_0 to $4m_P^2$.

All of the foregoing discussion, including Figs. 1 and 2, pertains to what can be called the familiar behavior of an anomalous threshold, in which the singularity emerges onto the physical sheet when analytic continuation in the masses is performed. Of course, for given fixed masses, the question whether the triangle diagram, Fig. 1(c), is singular on the physical sheet or not can be answered unambiguously and without recourse to mass continuation.

Questions of compositeness among the scalar and pseudoscalar mesons can be studied as functions of the chiral-symmetry breaking if we know how the masses of the S and P particles depend on the parameters describing the breaking. Because of the stability criteria associated with the different regimes of compositeness, we expect

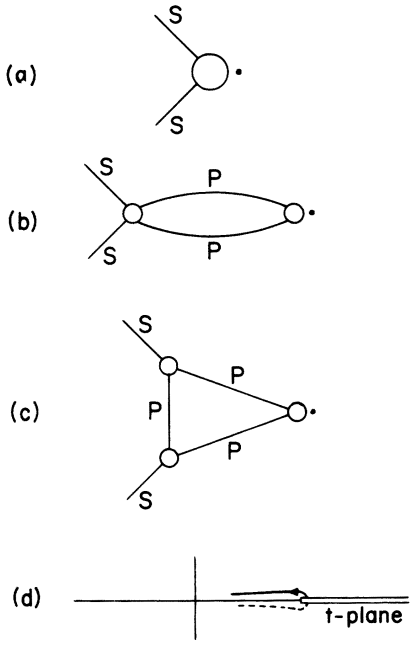

FIG. 1. Anomalous threshold where S is a bound state of PP. (a) S-particle form factor. (b) PP intermediate state. (c) Triangle contribution arising from the coupling $S \to PP$, and (d) giving a singularity which comes out of the PP cut onto the physical sheet as S becomes loosely bound.

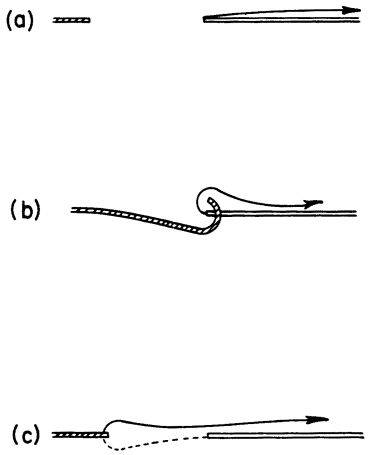

FIG. 2. Analytic continuation of the form factor. (a) Contour representation for the form factor when $m_S^2 < 2m_P^2$. The contour in Eq. (2) begins at the PP threshold. (b) As $m_S^2 \to 2m_P^2$, the singularity of the absorptive part deforms the contour. (c) For $m_S^2 > 2m_P^2$, the contour starting at the PP threshold has been deformed to include an anomalous contribution.

there to be peculiarities in these features when the theory which predicts the masses admits a Goldstone symmetry limit. We shall use the results of the CH investigation to provide expressions for the masses and so we expect the CH critical parameter to play a role in the manifestations of compositeness described by anomalous thresholds. We shall find that anomalous threshold properties are distinctly different above and below the critical value of the CH parameter.

II. SU(2)×SU(2) σ MODEL

This model has for its Lagrangian (apart from kinetic terms)

$$\mathcal{L} - \mathcal{L}_K = -\tfrac{1}{2}\mu^2(\sigma^2 + \vec{\pi}^2) + \tfrac{1}{4}f(\sigma^2 + \vec{\pi}^2)^2 - \epsilon\sigma, \qquad (3)$$

where $(\sigma, \vec{\pi})$ transform as $(\frac{1}{2}, \frac{1}{2})$ fields under SU(2)×SU(2), and for which we define $\xi = \langle 0|\sigma|0\rangle$. The parameters μ^2 and f are taken to be fixed while we permit ϵ and ξ to vary for the analysis of chiral-symmetry breaking. SU(2)×SU(2) invariance of the Lagrangian is broken by the term parametrized by ϵ. In addition there is chiral-symmetry breaking in the vacuum state for $\xi \neq 0$. If $\xi \to 0$ as $\epsilon \to 0$, we have a normal symmetry: The solution exhibits the symmetry of $\mathcal{L}$ and degenerate chiral multiplets result. If $\xi \not\to 0$ as $\epsilon \to 0$, we have a spontaneously broken symmetry and massless pions occur in the symmetry limit. The semiclassical solution of this model describes these properties in a way which depends on whether the critical parameter μ^2 is positive or negative.[5]

We follow CH and use

$$x = \xi/\hat{\xi}$$

and (4)

$$\lambda = \epsilon/(\hat{\xi}^3 f).$$

For $\mu^2 < 0$ we define[11] $\hat{\xi} = (\mu^2/f)^{1/2}$. Then the semiclassical solution relates x to λ (ξ to ϵ):

$$\lambda = x(x^2 - 1) \qquad (5a)$$

and determines the masses:

$$m_\pi{}^2 = \mu^2(1 - x^2)$$

and (6a)

$$m_\sigma{}^2 = \mu^2(1 - 3x^2).$$

For $\mu^2 > 0$ we define $\hat{\xi} = (-\mu^2/f)^{1/2}$ and obtain

$$\lambda = x(x^2 + 1), \qquad (5b)$$

$$m_\pi{}^2 = \mu^2(1 + x^2)$$

and (6b)

$$m_\sigma{}^2 = \mu^2(1 + 3x^2).$$

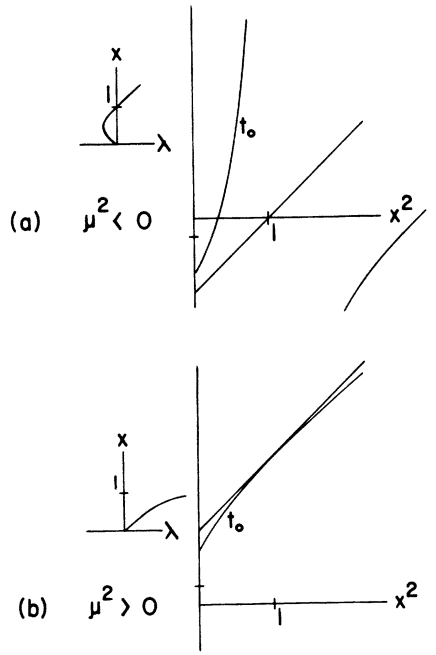

FIG. 3. Anomalous singularity t_0 and $\pi\pi$ threshold as functions of x^2 for (a) $\mu^2 < 0$ and (b) $\mu^2 > 0$. The scale marked on the ordinate is the value of μ^2. The straight line is the $\pi\pi$ threshold, $4m_\pi{}^2$; the anomalous curve has a point of tangency with it only in case (b). The insets show $x(\lambda)$ for each case; only in case (a) is there a Goldstone symmetry limit.

The forms taken by Eq. (1) in the two cases are

$$t_0 = \mu^2(3 - x^2)(1 - 3x^2)/(1 - x^2) \quad \text{for } \mu^2 < 0 \qquad (7a)$$

and

$$t_0 = \mu^2(3 + x^2)(1 + 3x^2)/(1 + x^2) \quad \text{for } \mu^2 > 0; \qquad (7b)$$

we have identified $S = \sigma$ and $P = \pi$ in Eq. (1) and, correspondingly, in Fig. 1.

Because of the substitution symmetry, (x, λ) for $(-x, -\lambda)$, we need only consider $x \geq 0$ and use x^2 as the variable on which the locations of the thresholds depend. In Fig. 3 we plot the $\pi\pi$ threshold, $4m_\pi{}^2$, and t_0 vs x^2 for case (a): $\mu^2 < 0$, and case (b): $\mu^2 > 0$. The insets to the figure show $x(\lambda)$ for each case. Only for $\mu^2 < 0$ is the Goldstone symmetry limit possible: $x \not\to 0$ as $\lambda \to 0$. On the other hand, only for $\mu^2 > 0$ does the anomalous threshold t_0 pass around the $\pi\pi$ threshold onto the physical sheet. The point of tangency between the two curves at $x^2 = 1$ in Fig. 3(b) indicates this: If we start with $x^2 \simeq 0$ and increase its value,[12] the anomalous singularity comes out of the $\pi\pi$ cut as in Fig. 1(d) and deforms the contour of the σ form factor as shown in Fig. 2. A rather different phenomenon takes place for $\mu^2 < 0$. In this case there is no tangency between the t_0 curve and the $4m_\pi{}^2$

curve. Thus, either t_0 never appears on the physical sheet or never disappears from it. The latter circumstance applies here,[12a] as can be seen by choosing a convenient fixed configuration of π and σ masses, say, for $x^2>3$.

We conclude that μ^2 is critical for governing the occurrence of not only the Goldstone symmetry limit, but also the familiar sort of anomalous threshold. These two phenomena are mutually exclusive. When μ^2 is such that the Goldstone limit can occur, the anomalous singularity which occurs is on the physical sheet but does not change sheets.

III. SU(3)×SU(3) σ MODEL

The Lagrangian is given by

$$\begin{aligned}\mathfrak{L}-\mathfrak{L}_K=&-\tfrac{1}{2}\mu^2\,\mathrm{Tr}M^\dagger M+f_1(\mathrm{Tr}M^\dagger M)^2\\&+f_2\,\mathrm{Tr}M^\dagger MM^\dagger M\\&+g\,(\det M+\mathrm{H.c.})-\epsilon_0\sigma_0-\epsilon_8\sigma_8\ .\end{aligned}\tag{8}$$

M is $(3,\bar{3})$ transforming under SU(3)×SU(3) and describes scalar and pseudoscalar fields, a nonet of each:

$$M=\sum_{k=0}^{8}(\sigma_k+i\phi_k)\lambda_k/\sqrt{2}\ .$$

Chiral-symmetry breaking is parametrized by ϵ_0 and ϵ_8, and by

$$\xi_0=\langle 0|\sigma_0|0\rangle$$

and

$$\xi_8=\langle 0|\sigma_8|0\rangle\ .$$

The authors of Refs. 1 and 3 have applied the semiclassical approximation to determine the relations among all the parameters and to solve for the masses of all the particles.[13] We shall use these results in Sec. IV, but for the present we are primarily interested in the expressions which hold for the special case of exact SU(3) symmetry. Accordingly, we shall develop our observations about compositeness in parallel with the CH treatment given in Sec. III of Ref. 5. For this case

$$\begin{aligned}&\epsilon_8=0\,,\\&\xi_8=0\,,\\&\epsilon_0/\xi_0=-\mu^2+4\xi_0^2(f_1+\tfrac{1}{3}f_2)+\gamma\xi_0\,,\quad \gamma=2g/\sqrt{3}\ .\end{aligned}\tag{9}$$

The scalar-particle masses, for octet and singlet, are

$$\begin{aligned}m_{S8}^2&=\mu^2-4\xi_0^2(f_1+f_2)+\gamma\xi_0\,,\\m_{S1}^2&=\mu^2-4\xi_0^2(3f_1+f_2)-2\gamma\xi_0\,;\end{aligned}\tag{10}$$

the pseudoscalar masses, similarly, are

$$\begin{aligned}m_{P8}^2&=\mu^2-4\xi_0^2(f_1+\tfrac{1}{3}f_2)-\gamma\xi_0\,,\\m_{P1}^2&=\mu^2-4\xi_0^2(f_1+\tfrac{1}{3}f_2)+2\gamma\xi_0\,.\end{aligned}\tag{11}$$

Following CH, we define

$$x=\xi_0/\hat{\xi}_0$$

and

$$\lambda=\epsilon_0/(\hat{\xi}_0^3 f)\,,\tag{12}$$

where

$$\hat{\xi}_0=-\gamma/f$$

and

$$f=4(f_1+\tfrac{1}{3}f_2)\,.$$

As in Sec. II, μ^2 is a critical parameter; Carruthers and Haymaker[5] choose to express the critical behavior in terms of τ, defined by

$$\tau=-4f\mu^2/\gamma^2\,.$$

In terms of these quantities, Eq. (9) becomes

$$\lambda=x[\,x(x-1)+\tfrac{1}{4}\tau\,]\ .\tag{13}$$

It suffices for us to consider the anomalous threshold of Fig. 1 for $S=S_1$ and $P=P_8$. For this case

$$\begin{aligned}m_P^2&=m_{P8}^2\\&=\mu_0^2(x^2-x+\tfrac{1}{4}\tau)\,,\\m_S^2&=m_{S1}^2\\&=\mu_0^2(3x^2-2x+\tfrac{1}{4}\tau)\,,\end{aligned}\tag{14}$$

where $\mu_0^2=4\mu^2/\tau=-\gamma^2/f$. Then, from Eq. (1) we get

$$t_0=\mu_0^2\,\frac{(x^2-2x+\frac{3}{4}\tau)(3x^2-2x+\frac{1}{4}\tau)}{x^2-x+\frac{1}{4}\tau}\ .\tag{15}$$

The location of the anomalous singularity (15) takes on a simpler appearance when we look at it from the PP threshold, as in Eq. (1′):

$$\begin{aligned}\nu_0&=t_0-4m_P^2\\&=-\mu_0^2\,\frac{(x^2-\frac{1}{4}\tau)^2}{x^2-x+\frac{1}{4}\tau}\ .\end{aligned}\tag{15′}$$

The zero of ν_0 for $x^2=\frac{1}{4}\tau$ is the feature of particular interest to us. In the series of drawings, Figs. 4(a) through 4(g), we plot the dependence on x of the anomalous singularity, t_0, and the PP threshold, $4m_P^2$. It is clear that, because of the larger number of parameters in the model, there are many distinct cases to consider, corresponding to different regimes for the critical parameter τ. Carruthers and Haymaker[5] have already noted τ's significance with respect to the behavior of $x(\lambda)$, Eq. (13); we have drawn $x(\lambda)$ as an inset in each of Figs. 4(a)–4(g). The substitution sym-

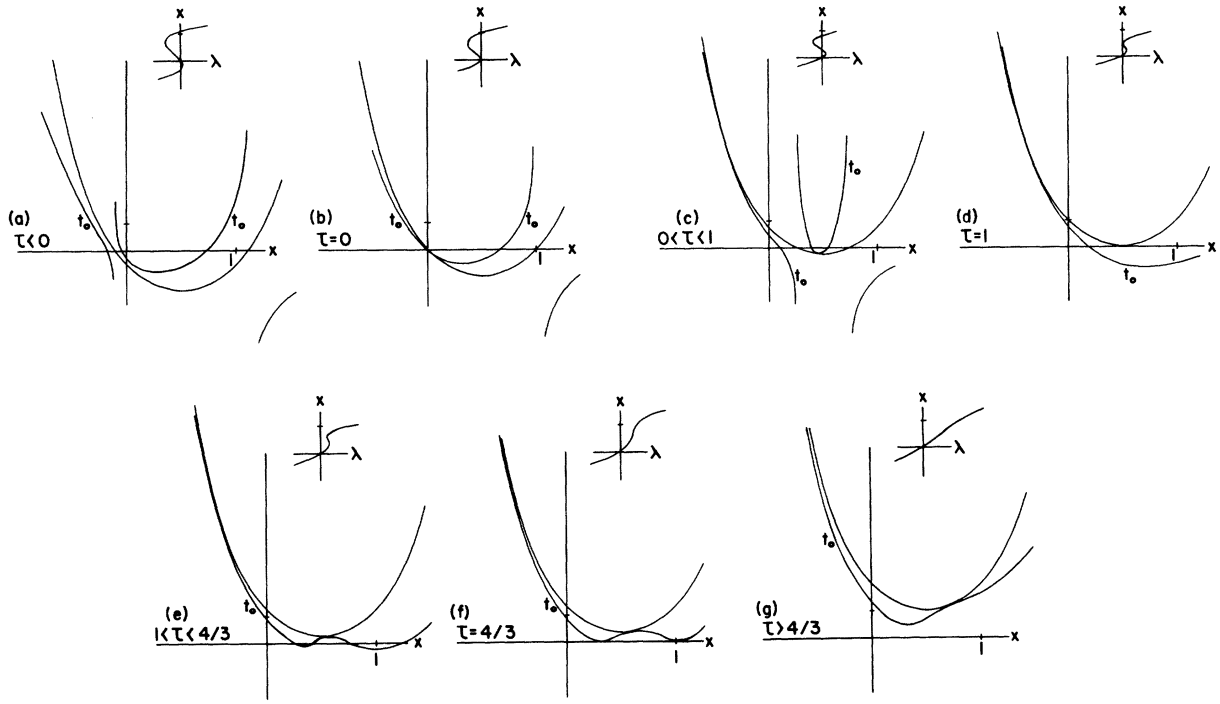

FIG. 4. Anomalous singularity t_0 and PP threshold as functions of x for (a) $\tau<0$, (b) $\tau=0$, (c) $0<\tau<1$, (d) $\tau=1$, (e) $1<\tau<\frac{4}{3}$, (f) $\tau=\frac{4}{3}$, and (g) $\tau>\frac{4}{3}$. The scale marked on the ordinate is the value of μ_0^2. The parabola in each case is the PP threshold, $4m_P^2$. The anomalous curve has a tangency with it, corresponding to a singularity changing sheets, only if $\tau>1$. The insets show $x(\lambda)$ for each case; only if $\tau\leq 1$ is there a Goldstone symmetry limit.

metry, (x,λ) for $(-x,-\lambda)$, found for SU(2)×SU(2), does not obtain here. However, even though positive and negative x are distinguishable, we still need consider only one or the other; as it turns out, $x\geq 0$ spans the range of x between the normal symmetry limit and the physical point, including the possible intervening occurrence of a Goldstone symmetry limit.

For orientation in reading Fig. 4, we make note of several special values of x:

(1) The normal symmetry limit, $x\to 0$, when $\lambda\to 0$, occurs for every τ.

(2) The Goldstone symmetry limit, in which $x\to x_\pm$ when $\lambda\to 0$, occurs for $\tau<1$:

$$x_\pm=\tfrac{1}{2}[1\pm(1-\tau)^{1/2}];$$

$m_P^2=0$ at these points.

(3) The points of tangency between t_0 and $4m_P^2$ arise where $x=\pm\frac{1}{2}\sqrt{\tau}$ and occur for $\tau>0$.

(4) The turning points in $x(\lambda)$ appear at $x=\bar{x}_\pm$ where $d\lambda/dx=0$:

$$\bar{x}_\pm=\tfrac{1}{3}[1\pm(1-\tfrac{3}{4}\tau)^{1/2}].$$

(5) The zeros of t_0, Eq. (15), are at $\bar{x}_+$, $\bar{x}_-$, $3\bar{x}_+$, and $3\bar{x}_-$; t_0 has singularities at x_+ and x_-.

The drawings may now be considered in turn to see the development of the anomalous threshold. A tangency of the t_0 curve from below the $4m_P^2$ curve is required for a singularity which changes sheets. As implied by the discussion in Sec. I, we must start increasing x from an initial value for which the PP cut is the lowest threshold. In general this means we start with $x\lesssim 0$ (the normal symmetry limit), increase x toward its physical value,[14] and see if t_0 deforms the contour which starts at the PP threshold.

Case (a) ($\tau<0$). There is no tangency so t_0 never passes through the PP cut.

Case (b) ($\tau=0$). t_0 crosses the PP threshold but does not deform the contour.

Case (c) ($0<\tau<1$). When we increase x, starting where $x\lesssim 0$, we see that $t_0\to-\infty$ (when $x\to x_-$). When t_0 returns to the finite plane (for $x_-<x<x_+$), it does not deform the contour below the PP threshold.

Case (d) ($\tau=1$). t_0 does not deform the contour as we proceed from $x\lesssim 0$. We note that this is the crucial value of τ above which the Goldstone symmetry limit no longer occurs.

Cases (e), (f), (g) ($\tau>1$). The t_0 curve has a tangency, from below, with the $4m_P^2$ curve at $x=\frac{1}{2}\sqrt{\tau}$. Correspondingly, the anomalous threshold comes out of the PP cut and deforms the contour.

The conclusion we draw is as in Sec. II. The critical parameter, referred to as τ in this model, controls the occurrence of the Goldstone symmetry limit and the emergence of the anomalous threshold. Again, these two phenomena are mutually exclusive. In cases (a) through (d), in which $\tau \leq 1$ admits the Goldstone limit, there is an anomalous singularity which never disappears from the physical sheet as x is varied.

IV. CONCLUSIONS

The parameters μ^2, f_1, f_2, and g of the chiral-symmetric part of (8) are taken to be fixed, so physical data ought to provide a determination of them and particularly of the critical parameter τ. We shall conclude this investigation with a physical fit to the SU(3)×SU(3) σ model, and express our version of the less-than-decisive results.[15]

As Olshansky[1] has done, we first determine the quantity b in terms of the decay constant ratio:

$$F_K/F_\pi = (1-\tfrac{1}{2}b)/(1+b), \quad b = \xi_8/(\sqrt{2}\xi_0).$$

Then from the known pseudoscalar meson masses we use m_π^2, m_K^2, and $\frac{1}{2}(m_\eta^2 + m_{\eta'}^2)$ to fix the quantities

$$m_0^2 = \mu^2 - 4f_1\xi_0^2(1+2b^2),$$

$$\Gamma = \gamma\xi_0,$$

and

$$y_2 = 4f_2\xi_0^2/(3\Gamma).$$

(Rather than reproduce all the formulas from the semiclassical approximation we refer the reader to the other authors.[13]) The pseudoscalar mixing angle is given by

$$\tan 2\theta_P = -2\sqrt{2}\,b\,\frac{1+y_2(2-b)}{3+2b-y_2b(2-b)}. \tag{16}$$

The procedure to this point determines θ_P and the masses of the pseudoscalars η and η', and of the scalars π_N and κ:

$$\begin{aligned}
&\theta_P = 0.87^\circ,\\
&m_\eta = 0.550\ \text{GeV}, \quad m_{\eta'} = 1.057\ \text{GeV},\\
&m_{\pi_N} = 1.015\ \text{GeV}, \quad m_\kappa = 1.026\ \text{GeV}.
\end{aligned}$$

Also determined are

$$\begin{aligned}
&m_0^2 = 0.351\ \text{GeV}^2,\\
&\Gamma = 0.319\ \text{GeV}^2,\\
&f_2\xi_0^2 = -0.0914\ \text{GeV}^2\\
&\epsilon_0/\xi_0 = -0.181\ \text{GeV}^2,\\
&\epsilon_8/(\sqrt{2}\xi_0) = 0.165\ \text{GeV}^2\\
&a = -0.911, \quad b = -0.157,
\end{aligned} \tag{17}$$

in which $a = \epsilon_8/(\sqrt{2}\epsilon_0)$.

The scalar mixing angle is given by

$$\tan 2\theta_S = 2m_{S08}^2/(m_{S00}^2 - m_{S88}^2)$$

$$= -2\sqrt{2}b\,\frac{1-y_1-3y_2(2-b)}{3+2b+y_1(1-2b^2)+3y_2b(2-b)}, \tag{18}$$

where $y_1 = 8f_1\xi_0^2/\Gamma$. Because the evidence on the isoscalar scalar mesons is not firm, we shall treat θ_S as a variable. Each choice of θ_S leads to a determination of the scalar masses m_ϵ and $m_{\epsilon'}$, and of $f_1\xi_0^2$, μ^2, and τ. To see the range over which θ_S can vary, it is useful to observe that because $\theta_P \simeq 0$ we have $y_2 \simeq -1/(2-b)$ and so

$$m_{S08}^2 \simeq \sqrt{2}\Gamma b(4-y_1),$$

$$m_{S00}^2 - m_{S88}^2 \simeq -\Gamma[3-b+y_1(1-2b^2)].$$

Then when we examine (18) we find that θ_S lies in the range

$$90^\circ + \theta_0 < \theta_S < 180^\circ + \theta_0,$$

where $\theta_0 = \tan^{-1}(\sqrt{2}b)$, a negative angle. A portion of this range gives very realistic values for m_ϵ and $m_{\epsilon'}$. In Fig. 5 we have plotted the results $m_{\epsilon,\epsilon'}$ and τ as functions of θ_S.

We would like to be able to say that a physical fit is possible which determines τ and tells us which of the circumstances drawn in Fig. 4 actually applies. We see from Fig. 5, however, that

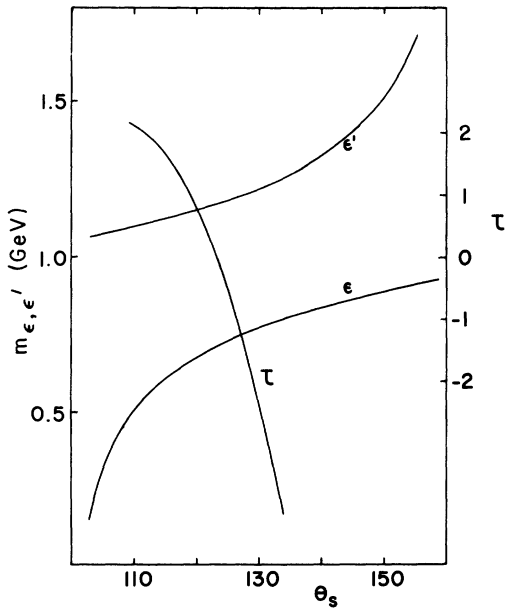

FIG. 5. Calculated masses (in GeV) of the isoscalar scalar mesons ϵ and ϵ', and the critical parameter τ vs the scalar mixing angle θ_S (in degrees).

we can conclude rather little. The simplified model has given values of m_ϵ and $m_{\epsilon'}$ which are realistic over a range of θ_S, but over that range τ varies through all of the regimes considered in Fig. 4. Were we to choose the ϵ meson to be at 700 MeV, we would have

$$\theta_S = 122^\circ,$$
$$m_\epsilon = 0.700 \text{ GeV}, \quad m_{\epsilon'} = 1.162 \text{ GeV},$$
$$\mu^2 = 0.0190 \text{ GeV}^2, \tag{19}$$
$$f_1 \xi_0^2 = -0.0791 \text{ GeV}^2,$$
$$\tau = 0.329.$$

If we pursue this, and in addition determine the physical value of ξ_0 from F_π by means of

$$F_\pi = (\tfrac{2}{3})^{1/2} \xi_0 (1+b),$$

we get

$$\xi_0 = 0.137 \text{ GeV},$$
$$f_1 = -4.23, \quad f_2 = -4.88, \quad \gamma = 2.33 \text{ GeV},$$
$$\epsilon_0 = -0.0248 \text{ GeV}^3, \quad \epsilon_8/\sqrt{2} = 0.0226 \text{ GeV}^3.$$

This also fixes the parameters introduced in Sec. III:

$$f = -23.44, \quad \hat{\xi}_0 = 0.0995 \text{ GeV}.$$

The physical point to which we referred in the discussion of Fig. 4 therefore has coordinates

$$x = 1.373, \quad \lambda = 1.072.$$

This choice of physical fit, with $\tau = 0.329$, would imply that Fig. 4(c) is applicable, for which $0 < \tau < 1$; unfortunately, τ is too sensitive to the choice of m_ϵ and the evidence for an observed ϵ meson is too tentative to permit us to give that much credence to (19).

The physical fit has not given a definitive answer within this model to the question of the realization of chiral symmetry. Nor has it revealed which case shown in Fig. 4 is really applicable. These failings notwithstanding, the primary observations of this study are still interesting. If the scalar mesons can be thought of as composites of a pair of pseudoscalar mesons, then a loosely bound configuration ought to be possible as the masses are varied. On the other hand, the stability criteria for anomalous thresholds may have peculiar consequences if the system possesses a Goldstone symmetry with massless pseudoscalar mesons occurring in the limit. The model makes a clean distinction: The parameters of the symmetric part of the Lagrangian can permit a Goldstone symmetry limit or an anomalous threshold which changes sheets, but these phenomena are mutually exclusive. When the parameters admit a Goldstone limit, the anomalous singularity is one which never leaves the physical sheet. The critical parameter controlling this distinction is μ^2 (equivalently, τ). Carruthers and Haymaker[5] have conjectured that μ^2 behaves like a critical temperature for a system near a phase transition. The observations we have made in this study offer further evidence of distinctly different behavior above and below the critical point.

---

*Work supported in part by the National Science Foundation.

[1]R. Olshansky, Phys. Rev. D 4, 2440 (1971).
[2]M. Gell-Mann and M. Lêvy, Nuovo Cimento 16, 705 (1960); M. Lêvy, *ibid.* 52A, 23 (1967).
[3]P. Carruthers and R. W. Haymaker, Phys. Rev. D 4, 1808 (1971).
[4]As part of a study of the renormalization of the model, the one-closed-loop corrections have been calculated and are found to be small, giving more credence to the semiclassical results: L.-H. Chan and R. W. Haymaker, Phys. Rev. D 7, 402 (1973).
[5]P. Carruthers and R. W. Haymaker, Phys. Rev. D 6, 1528 (1972).
[6]We shall not need to consider the tightly bound case for which m_S is small enough such that the *SS* intermediate state has a threshold lower than *PP*.
[7]R. Karplus, C. M. Sommerfield, and E. H. Wichmann, Phys. Rev. 111, 1187 (1958).
[8]For a general review, see R. J. Eden, in *Lectures in Theoretical Physics*, proceedings of the 1961 Brandeis Summer Institute (Benjamin, New York, 1962), Vol. 1, p. 1.
[9]Y. Nambu, Nuovo Cimento 9, 610 (1958); R. Blankenbecler and Y. Nambu, *ibid.* 18, 595 (1960).
[10]S. Mandelstam, Phys. Rev. Lett. 4, 84 (1960); R. E. Cutkosky, *ibid.* 4, 624 (1960); R. Blankenbecler and L. F. Cook, Phys. Rev. 119, 1745 (1960); J. J. Brehm, Ann. Phys. (N.Y.) 25, 221 (1963).
[11]f is negative.
[12]Actually, for $x^2 = 0$ the $\sigma\sigma$ and $\pi\pi$ cuts start together. For $x^2 > 0$ the $\sigma\sigma$ cut moves to the right faster than the $\pi\pi$ cut does, so that it has no influence.
[12a]The author thanks R. W. Haymaker for correcting his observation on this point.
[13]See Table I of Ref. 3 and footnote 23 of Ref. 5. The μ^2 terms, left out in Ref. 3, are trivially instated. See also Table I of Ref. 4.
[14]Anticipating a later result, the physical value of x is greater than 1.
[15]See also Refs. 1, 3, 4, and 5.